The Influence of Mounting Angle on Gurney Flap on The Aerodynamics Performance of NACA 0015 Using CFD Method

Mirza Fauzan Lukiano[1], James Julian [2], Fitri Wahyuni [3] Waridho Iskandar [4]

Abstract— **Improving the airfoil aerodynamics is quite an essential aspect of the aviation industry. One method for improving airfoil aerodynamics involves applying passive flow control techniques. The effect of using the gurney flap as passive flow control was explored through the CFD approach with the RANS control equation and incorporating k-epsilon as a turbulence model. The airfoil model utilized in this study was the NACA 0015 airfoil operating at a Reynolds number of 1×10^6. This study explored three different mounting angles of the gurney flap, namely 45°, 60°, and 90°. The outcomes show that adding the gurney flap has positive results in increasing the lift and drag of the NACA 0015. An airfoil with a mounting angle flap of 45° has an average percentage increase in C_l of 23%, followed by a mounting angle flap of 60°, which is 28%, and a percentage C_l of 45% for a mounting angle flap of 90°. Meanwhile, Gurney flaps with a mounting angle of 45° can increase C_d by an average percentage of 3%, while mounting angle flap at 60° increases the C_d percentage by 4% and 5% for a mounting angle of 90°. Moreover, fluid flow visualization with pressure and velocity contours was given at AoA 10º to determine its effect on increasing lift and drag on the NACA 0015 airfoil.**

Keywords—**NACA 0015, CFD, Gurney flap, Mounting angle, Aerodynamics performance**

I. INTRODUCTION

Aircraft wings are one of the most essential components in the aviation industry. This is because the aerodynamic characteristics of aircraft wings directly impact the aircraft's performance and efficiency. For example, during takeoff, flight control, and flight range [1]. Therefore, it is essential to carry out developments to increase lift and reduce drag force but still pay attention to ease of application and not cause excessive energy expenditure [2]. Various methods can be used, one of which is using a passive fluid control device. A passive flow control device is a control device that is capable of manipulating fluid flow by changing the geometric profile of an object, which, in this case is an airfoil [3]. Various types of passive fluid flow control devices are applied to airfoils to improve aerodynamic performance, and one is by adding a gurney flap.

Gurney flap (GF) is a simple but effective passive flow control method to improve aerodynamic performance [4]. This device was introduced by American car racing legend Dan Gurney in 1971 [5]. Initially, this innovation found its application in the realm of racing cars as a petite vertical strip affixed to the trailing edge of the wing [6][4]. Various studies have been performed to understand the performance of airfoils with Gurney flaps and their application to aircraft and helicopters [7][8].

To understand the aerodynamic improvements produced by the Gurney flap, Liebeck initiated experimental investigations of the gurney flap characteristics in the wind tunnel. The results showed an addition in lift force at each AoA on the airfoil that had the gurney flap installed, making a difference from the baseline airfoil [9]. Meanwhile, Storms and Jang investigated a similar phenomenon in experiments employing a NACA 0012 airfoil, utilizing a GF with a height of 0.5%c. The results obtained the best aerodynamic efficiency at this flap size with increased lift and drag coefficients [10].

Other research used CFD to optimize gurney flaps on NACA 4312 airfoils with a Reynolds number of 5×10^5. The flap height is 1.5% to 3% of the airfoil length for different AoA (0° - 16°). The conclusion obtained from this investigation indicates that the peak lift and drag ratio is attained at an AoA of 4° for all flap lengths, with the flap featuring a length of 1.5% of the airfoil chord demonstrating the most advantageous aerodynamic performance [7]. Then, another study was conducted using computing to test the effect of the gurney flap on the NACA 0012 with variations in the height and location of the GF from the trailing edge. The results show that a 0.015 h/c GF achieved the highest lift coefficient [11]. Also, similar results were obtained when numerical analysis was conducted on the NACA 4412 airfoil by altering both the AoA and GF heights, spanning from 0.5%c to 2.5%c. The results indicate that the 1.5%c delivered the highest lift-to-drag ratio [12].

Studies on using the Gurney flap as a passive fluid flow control device have been carried out experimentally and computationally. The results show that this passive control device's characteristics of size, position, and geometric shape still influence improving aerodynamic performance. Therefore, further development regarding

Mirza Fauzan Lukiano, Departement of Mechanical-Engineering, Universitas Pembangunan Nasional Veteran Jakarta, Jakarta, 12450, Indonesia. E-mail: mirza.fl@upnvj.ac.id.

James Julian, Departement of Mechanical Engineering, Universitas Pembangunan Nasional Veteran Jakarta, Jakarta, 12450, Indonesia. E-mail: zames@upnvj.ac.id.

Fitri Wahyuni, Departement of Mechanical Engineering, Universitas Pembangunan Nasional Veteran Jakarta, Jakarta, 12450, Indonesia. E-mail: fitriwahyuni@upnvj.ac.id.

Waridho Iskandar, Fluid Mechanics Laboratory, Universitas Indonesia, Kampus Baru UI, Depok, 16424, Indonesia. E-mail: waridho.iskandar@ui.ac.id.

International Journal of Marine Engineering Innovation and Research, Vol. 8(4), Dec. 2023. 694-702
(pISSN: 2541-5972, eISSN: 2548-1479)

695

this passive control device is still needed to achieve maximum efficiency. The focus of this study is on the optimization of the NACA 0015 through the addition of a gurney flap as a passive fluid flow control device. The computational approach was executed at a Reynolds number of 10^6. Then, variations in the Gurney flap mounting angles were proposed to determine the maximum level of aerodynamic efficiency on the NACA 0015 airfoil.

gurney flap with mounting angles of 45º, then the third and fourth variations are gurney flaps with mounting angles of 60º and 90º. The gurney flap variation used in this study is placed on the trailing edge, with the width of each gurney flap being 0.05%c and the flap height 2%c. Various geometric model variations are created in semicircular and rectangular fluid domains. These domains were chosen because they can facilitate the creation of structured meshes. In this way, the computing
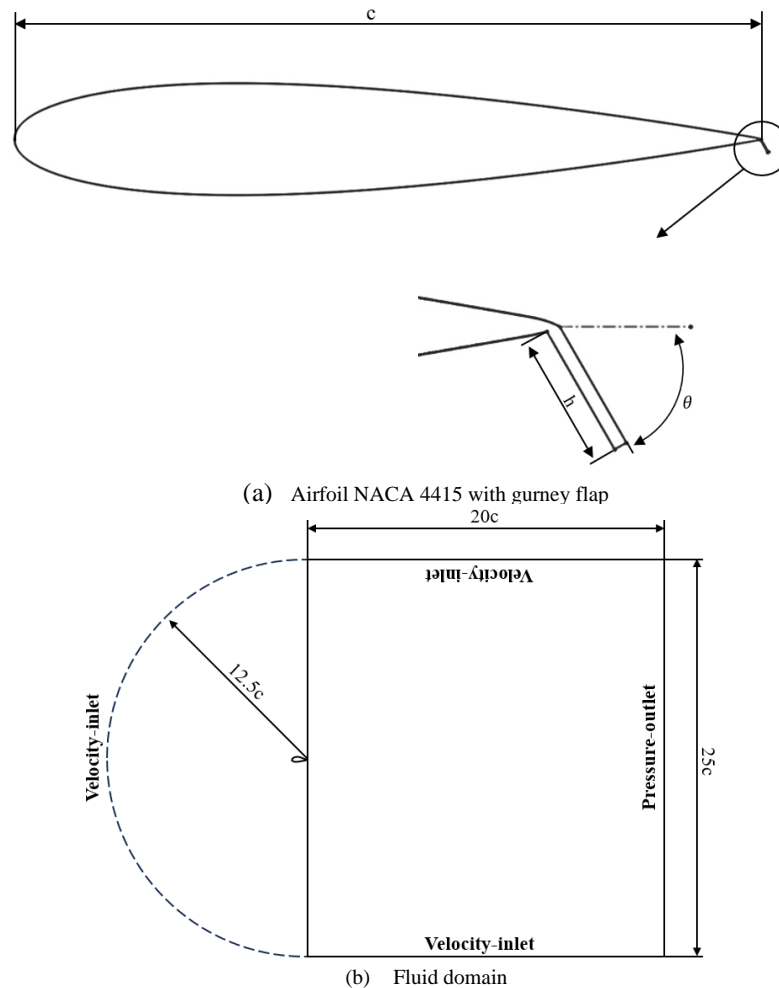

(a) Airfoil NACA 4415 with gurney flap

(b) Fluid domain

Figure 1. Detail geometry

II. METHOD

A. NACA 0015

The National Advisory Committee on Airfoils (NACA) four-digit series NACA 0015 is used by the airfoil [13]. In general, the own differentiation of "NACA" can be determined from the numbers. The NACA 0015 is symmetrical and has no chamber, as denoted by The first two digits, '00', and a thickness-to-chord length ratio (t/c) of 15%, as indicated by the number '15' [14]. The length of chord NACA 0015 employed is 1 meter.

B. Geometry configuration

In this study, two airfoil geometric models were generated: baseline NACA 0015 and NACA 0015 with a Gurney flap. Then, three variations of mounting angle gurney flap will be investigated in this study. The first variation is without using a gurney flap, the second is a

process becomes more accurate and efficient. Furthermore, the boundary conditions within these domains were categorized into velocity inlet and pressure outlet conditions. The airfoil's surface was governed by the no-slip wall boundary condition. Overall, detailed geometry and domains in this study are shown in Figure 1.

C. Governing equations

In this study, the governing Equation employed for incompressible fluid flow analysis is the Reynolds Averaged Navier Stokes (RANS), which consists of two key components, including the momentum and continuity equation. These RANS equations are detailed with different functions in Equation 1 and Equation 2 [15].

International Journal of Marine Engineering Innovation and Research, Vol. 8(4), Dec. 2023. 694-702
(pISSN: 2541-5972, eISSN: 2548-1479)

696

$$\frac{\partial p}{\partial t}\left(\rho u_i u_j\right) + \frac{\partial}{\partial x_i}\left(\rho u_i\right) =$$

$$\frac{\partial p}{\partial x_i} + \frac{\partial}{\partial x_j}\left[\mu\left(\frac{\partial u_i}{\partial x_j} + \frac{\partial u_j}{\partial x_i} - \frac{2}{3}\delta_{ij}\frac{\partial u_i}{\partial x_i}\right)\right] + \qquad (1)$$

$$\frac{\partial}{\partial x_i}\left(-\overline{\rho u_i' u_j'}\right)$$

$$\frac{\partial p}{\partial t} + \frac{\partial}{\partial x_i}\left(\rho u_i\right) = 0 \qquad (2)$$

In this study, we have selected the k-ε model as the turbulence model because of its accurate prediction capability for aerodynamic forces. Equations 3 and 4 present the mathematical equations of the k-ε turbulence model. [16].

$$\frac{D}{Dt}\left(\rho k\right) = \frac{\partial p}{\partial x_i}\left[\left(\mu + \frac{\mu_i}{\sigma_k}\right)\frac{\partial k}{\partial x_i}\right] + G_k - \rho\varepsilon \qquad (3)$$

$$\frac{D}{Dt}\left(\rho\varepsilon\right) = \frac{\partial p}{\partial x_j}\left[\left(\mu + \frac{\mu_i}{\sigma_\varepsilon}\right)\frac{\partial\varepsilon}{\partial x_j}\right]$$

$$+C_{el}\frac{\varepsilon}{k}G_k - \rho C_{\varepsilon 2}\frac{\varepsilon^2}{k} \qquad (4)$$

D. Aerodynamics forces

Aerodynamic forces generally found on airfoils play a role in determining the behavior of the airfoil when interacting with fluids. When an airfoil moves through a fluid, the two main aerodynamic forces that occur are drag and lift force. The drag force aligns with the fluid flow direction, while the force that acts perpendicular to the fluid flow direction is named the lift force. Therefore, it is essential to know and understand the behavior of airfoils, which is done to assist in selecting and designing

an effective and efficient control system. Generally, each is denoted as coefficient drag (C_d) and coefficient lift (C_l). These two equations are seen in equations 5 and 6 [17].

$$C_d = \frac{2d}{\rho u^2 c} \qquad (5)$$

$$C_l = \frac{2l}{\rho u^2 c} \qquad (6)$$

E. Mesh independence test

After completing the geometry setting stage, the next step is the meshing process. This stage is a computational process where the geometric domain is divided into small elements for the calculation process. A structured mesh is employed as the chosen element type in this study. Subsequently, three distinct mesh variations are employed: the first is a coarse mesh with 25000 elements, the second is a medium mesh with 50000 elements, and the last is a fine mesh with 100000 elements. All these mesh elements are arranged in a rectangular shape. Following this, the mesh is adjusted to be closer to the airfoil surface, facilitating the observation of diverse fluid flow phenomena nearby. Detailed information regarding these mesh variations is provided in Figure 2.

After the meshing process, the next step is to test mesh variations with a mesh independence test. This is done to ensure that the mesh used has a small error value so that it can be said to be the most efficient. Richardson's extrapolation method was the foundation for conducting this mesh independence test [18]. The sample mesh
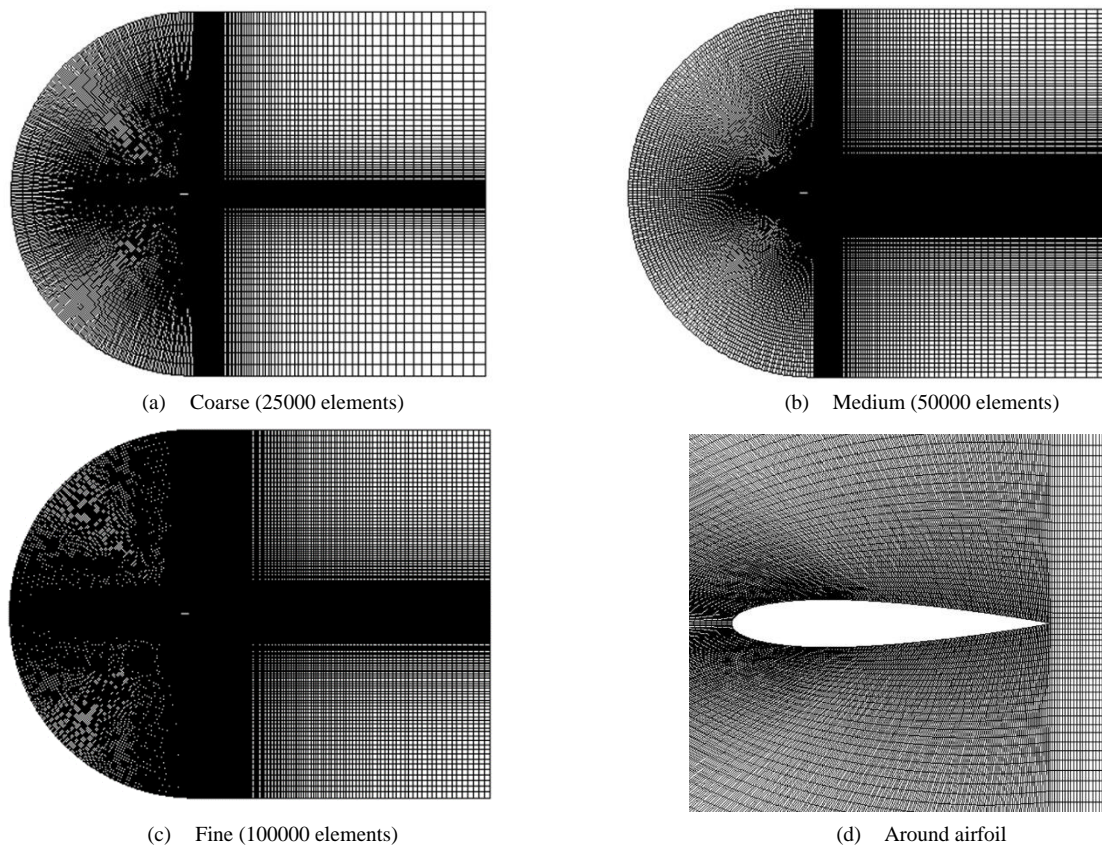

(a)   Coarse (25000 elements)

(b)   Medium (50000 elements)

(c)   Fine (100000 elements)

(d)   Around airfoil

Figure 2. Mesh in this study

independence test involves extracting velocity data, specifically at reference point x = 0.5 and y = 0.15 [19]. The initial stage in this process is to determine the variation ratio of the mesh elements that will be used with Equation 7. Then, determine the order value using Equation 8. In the next stage, the Grid Convergence Index (GCI) is carried out, which is divided into two, namely GCI coarse in Equation 9, which is the result of the error medium and coarse mesh variations, and GCI fine, defined in Equation 10, characterizing the error assessment the fine and medium mesh variations. The GCI results that have been determined are then analyzed using Equations 11 and 12 to guarantee that the mesh variations used are within a congruent range or are still in the best mesh category so that they can be used in this study [20]. Based on the test results, the mesh variations align with the convergence index range, proven by the results close to 1. The determination of the optimal grid count is based on the identification of the lowest error value. Thus, the entire computational process will utilize the fine mesh configuration. Overall mesh independence test results are given in Table 1.

$$r = \frac{h_2}{h_1} \tag{7}$$

$$\bar{p} = \frac{\ln\left(\frac{f_{fine} - f_{medium}}{f_{medium} - f_{coarse}}\right)}{\ln(r)} \tag{8}$$

$$GCI_{coarse} = \frac{F_s |\epsilon_{coarse}| r^{\bar{p}}}{\left(r^{\bar{p}} - 1\right)} \tag{9}$$

$$GCI_{fine} = \frac{F_s |\epsilon_{fine}|}{\left(r^{\bar{p}} - 1\right)} \tag{10}$$

$$\frac{GCI_{fine}}{GCI_{coarse} r^{\bar{p}}} \approx 1 \tag{11}$$

$$f_{rh=0} = f_{fine} + \frac{\left(f_{fine} - f_{medium}\right)}{\left(r^{\bar{p}} - 1\right)} \tag{12}$$
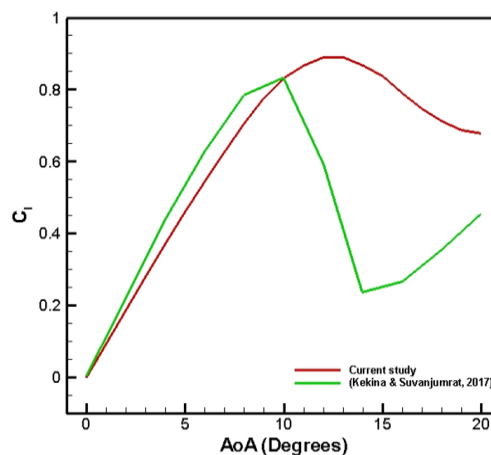
III. RESULT AND DISCUSSION
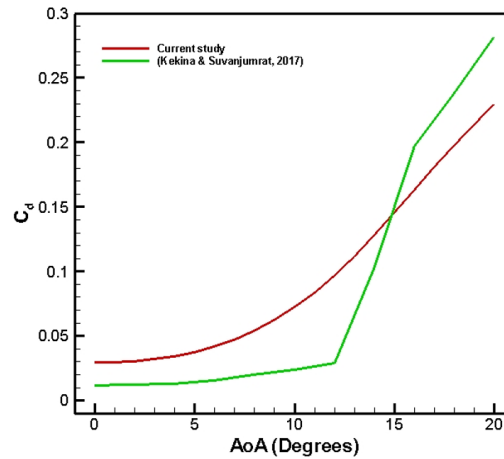
A. Data validation

Validation is conducted to ensure that all computing processes have been carried out correctly. Validation was taken out at a Reynolds number of 160000. This validation process employed experimental data from Kekina [21] and involved comparisons with the baseline data for the NACA 0015 airfoil. The validation results can be shown in Figure 3. Comparing the data for both C_l and C_d shows similarities in curve trends. However, there is a slight difference in the C_l curve, which lies in the stall condition in the experimental calculation, which shows the results are 1 degree faster, namely at AoA=10°, different when compared to the computational data at AoA=12°. Then, there is a difference after the stall condition, and this is because the airfoil data is difficult to predict after the stall condition. Meanwhile, examining the C_d curve reveals no substantial difference between the two datasets. In both cases, there is an increase in C_d along with an increase in AoA. Thus, it

can be inferred from comparing the two data that the computational data used is valid.

TABLE 1.
MESH INDEPENDENCE TEST RESULTS

Variation	Coarse	Medium	Fine
Velocity	40.3069	40.4237	40.4496
$f_{rh=0}$		40.456979648	
r		2	
p		2.173016271	
GCI_{coarse}		0.1029%	
GCI_{fine}		0.023%	
Results		1.000468	
Mesh errors	0.3710%	0.0823%	0.0182%

(a)   Plot of C_l against changes in AoA

International Journal of Marine Engineering Innovation and Research, Vol. 8(4), Dec. 2023. 694-702
(pISSN: 2541-5972, eISSN: 2548-1479)

698

(b)   Plot of Cd against changes in AoA

**Figure. 3.** Aerodynamics Validation

B. Analysis

The gurney flap can provide additional lift on the airfoil as a passive flow control device. This can be seen in Figure 4(a), which explains the increase in lift coefficient obtained by varying the installation angle, namely 45°, 60°, and 90°. At the gurney flap 45°, there is an increase in C_l with the top lift point condition, namely at AoA 11°. Also, when the mounting angle is increased to 60°, the maximum lift is obtained at AoA 10°. Meanwhile, the maximum lift value at AoA 11° is when the mounting angle is increased to 90°. The effect of the flap substantially increases the optimum lift coefficient. Compared to the NACA 0015 without flap, if the percentage increase in C_l is averaged, a mounting angle of 45° can increase the average percentage of C_l to 23%. In contrast, a mounting angle of 60° increases the average percentage of C_l by 28%, and a 90° mounting angle can increase the average percentage of C_l values by 45%. Overall, the increase in the average percentage increased significantly because it was influenced by the increase in C_l values in the low AoA range.

On the other hand, using gurney flaps tends to increase the drag coefficient along with increasing mounting angle size, especially at high angles of attack. Increasing C_d provides advantages in aerodynamic applications, one of which is aircraft. It can delay the movement of the aircraft when landing on a track that is not too wide. Besides that, it also helps maintain stability in certain

situations [22]. The influence of using the Gurney flap along with increasing the mounting angle is depicted in Figure 4(b). The variation in mounting angle reveals that the escalation in C_d commences at initial Angle of Attack (AoA) values, specifically within the AoA range of 0° - 7°, where a more substantial AoA, a more significant increase in C_d. Meanwhile, in the AoA range of 8° - 14°, there was a decrease in the resulting C_d value at a mounting angle of 90° when compared to variations in mounting angles of 45° and 60° which tended to experience an increase in the C_d value. Then, the divergence in Cd values generated by airfoils with varying mounting angles of 90° increases again, which starts to appear at AoA ≥15°. Overall, adding a passive gurney flap control device with varying mounting angles can increase the drag coefficient value, which is different from the baseline airfoil. Based on the average percentage increase in the C_d value produced, there was an increase in the C_d value of 3% when the gurney flap was installed with a mounting angle of 45°, then when the size of the mounting angles was increased again to 60° the percentage increase in C_d increased significantly to 4%, and continues to experience an increase in the percentage of C_d values of up to 5% when compared to the baseline airfoil if the mounting angles are increased to 90°.

Figure 5 has been constructed to ascertain the optimal AoA. Within the lift-to-drag curve, the optimal AoA is
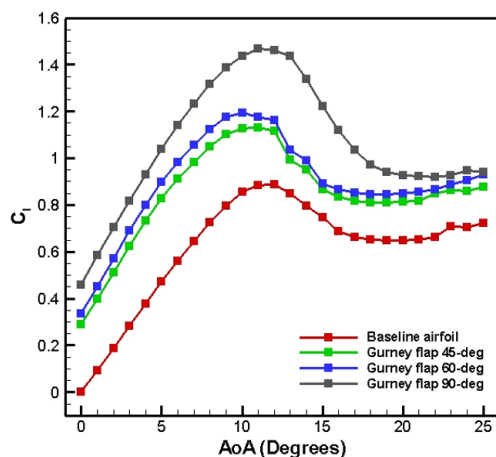
(a)   Plot of C_l against changes in AoA
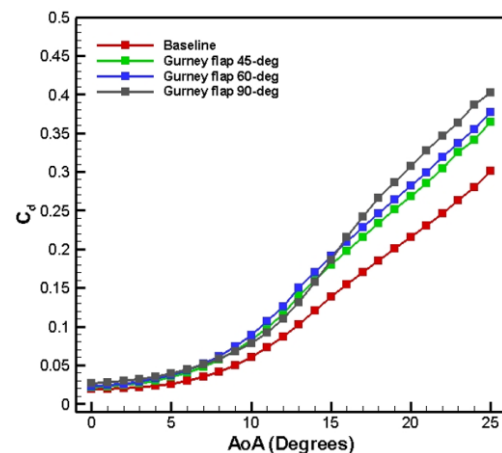
(b)   Plot of *Cd* against changes in AoA

Figure. 4. Aerodynamics force of NACA 0015

discerned as the highest point on the AoA curve. In the case of the baseline airfoil, the optimal AoA corresponds to 6°. Employing a gurney flap with 45° mounting angles produces the same optimal AoA, namely AoA 4°, while using a gurney flap with 60° mounting angles can speed up the optimal AoA to 6°. Also, if the mounting angles increase again to 90°, the optimal AoA will be 5°. The peak of the curve on the gurney flap with 90° mounting angles is the highest among the others. This is because the resulting increase in C_l and C_d is insignificant. However, different things were shown in the mounting angles of 45° and 60° where the initial However, different things were shown in the mounting angles of 45° and 60° where the initial trend of the curve showed positive results at the beginning but slowly

pressure coefficient at an AoA of 4 degrees is presented, as depicted in Figure 6. Compared with the baseline airfoil, the trend of the C_p curve in the upper and lower chambers shows an increase with each variation of the mounting angle. However, the distance between C_p on the upper and lower chamber airfoil differentiates each variation, especially on the trailing edge. When the GF is attached to the airfoil with a 90° mounting angle, it shows a significant increase in C_p at the trailing edge, which is different from other mounting angle variations. Thus, using a gurney flap with varying mounting angles effectively produces the highest C_l value at a mounting angle of 90°.

The difference in velocity distribution at the bottom and top is explained in the velocity contour visualization
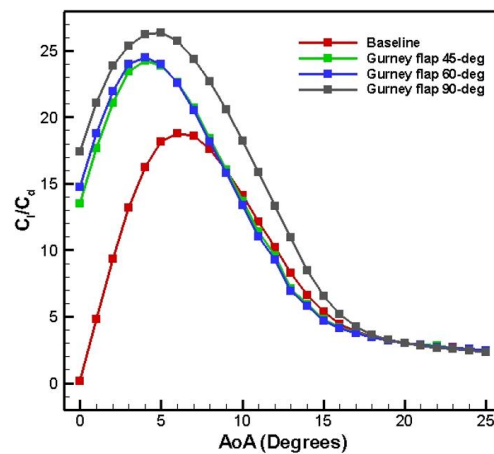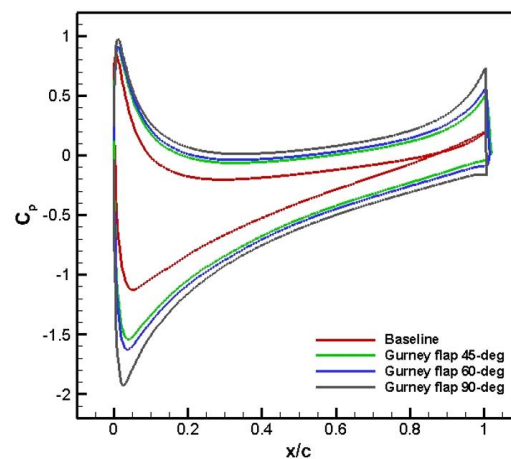

Figure 5. Graph ratio between C_l to C_d

Figure 6. Pressure distribution (changing mounting angles,
α = 4 deg)

decreased at AoA ≥5°. This decrease is influenced by C_d, which is more dominantly obtained at this mounting angle. Thus, based on the results of this analysis, using a Gurney flap featuring a 90° mounting angle is more recommended than other mounting angle variations.

To further analyze the role of installing a gurney flap on the trailing edge NACA 0015. The distribution of

in Figure 7. The samples used in this visualization were taken at AoA = 10°. Based on velocity contour analysis, the gurney flap also changes the fluid flow velocity in both the upper chamber and lower chamber airfoil. The upper fluid flow has increased quite significantly.
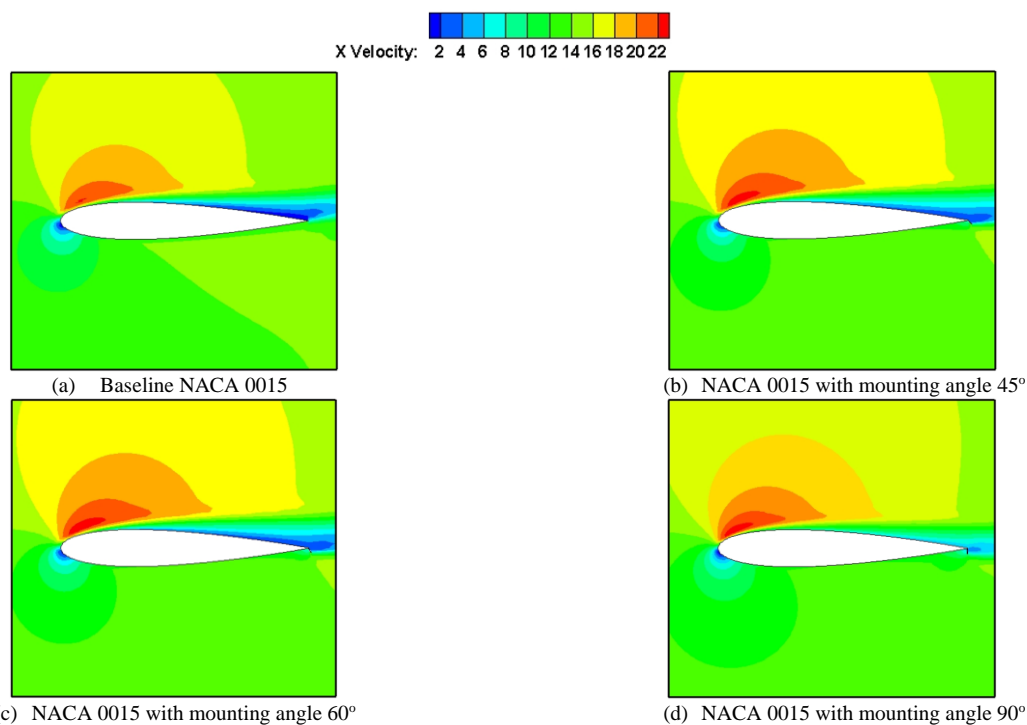
International Journal of Marine Engineering Innovation and Research, Vol. 8(4), Dec. 2023. 694-702
(pISSN: 2541-5972, eISSN: 2548-1479)

700

(a)   Baseline NACA 0015

(b)   NACA 0015 with mounting angle 45°

(c)   NACA 0015 with mounting angle 60°

(d)   NACA 0015 with mounting angle 90°

Figure. 7. Velocity contour at AoA 10°

(a)   Baseline NACA 0015

(b)   NACA 0015 with mounting angle 45°

(c)   NACA 0015 with mounting angle 60°

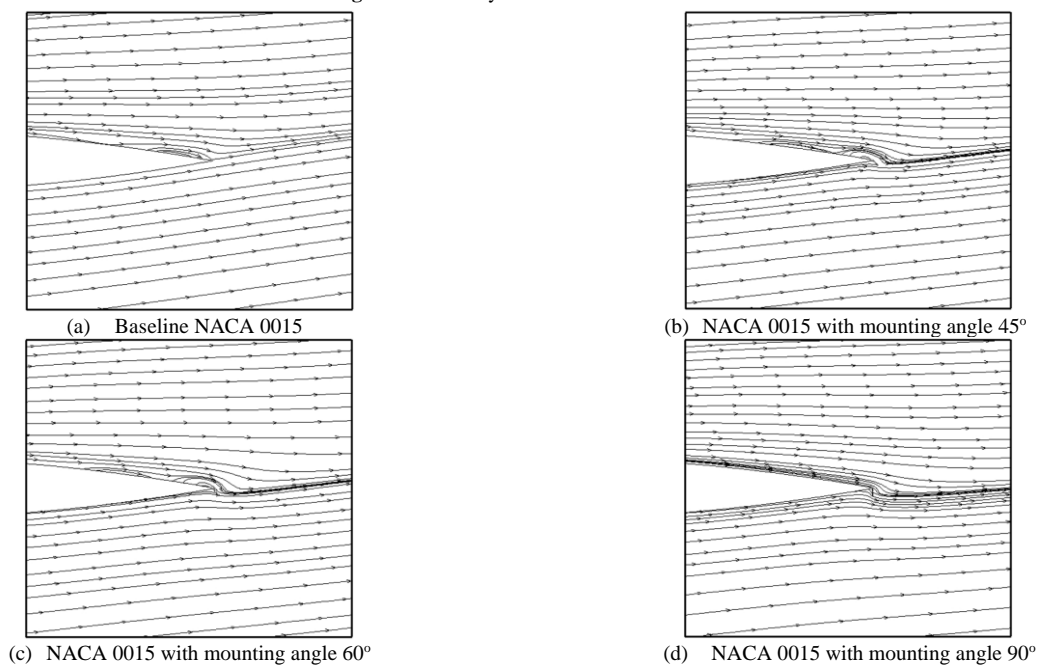(d)   NACA 0015 with mounting angle 90°

Figure. 8. Streamline contour at AoA 10°

However, this increase is of course different for each variation of mounting angle. The larger the mounting angle provided, the wider the high-velocity area. Conversely, the gurney flap causes fluid flow under the airfoil to decrease. This decrease will be more significant as the size of the mounting angle on the airfoil increases. On the other hand, the streamlined contour of the trailing-edge, as depicted in Figure 8, illustrates that using a gurney flap does not significantly affect fluid flow surrounding the airfoil. Therefore, increasing the performance of the NACA 0015 by using this fluid flow control device is entirely influenced by the pressure difference in the upper and lower chambers.

Meanwhile, another contour used in this study is the pressure contour shown in Figure 9. Like the velocity contour, the pressure contour sample was also taken at AoA = 10°. The gurney flap changes the upper and lower airfoil chamber pressure. The upper airfoil fluid flow experienced a significant decrease. This decrease occurred with each variation. The larger the mounting angle given, the wider the low-pressure area. On the other hand, mounting angle causes the lower airfoil fluid flow to increase. This increase will be more significant as the mounting angle size of the airfoil increases. Overall, the difference in lower and upper chamber pressure causes the airfoil to experience an increase in C_l.
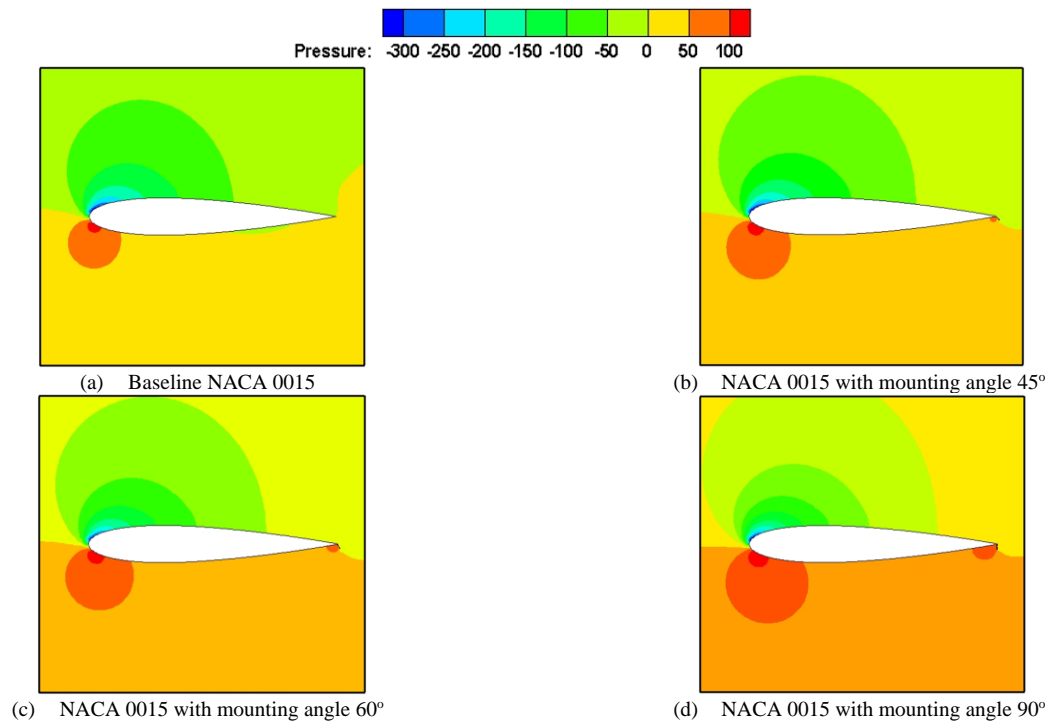
International Journal of Marine Engineering Innovation and Research, Vol. 8(4), Dec. 2023. 694-702
(pISSN: 2541-5972, eISSN: 2548-1479)

701

Pressure: -300 -250 -200 -150 -100 -50 0 50 100

(a) Baseline NACA 0015

(b) NACA 0015 with mounting angle 45°

(c) NACA 0015 with mounting angle 60°

(d) NACA 0015 with mounting angle 90°

Figure. 9. Pressure contour at AoA 10°

IV. CONCLUSION

In this study, the primary focus is investigating the aerodynamic characteristics of the NACA 0015. An improvement in the Cl and Cd values produced by the airfoil was achieved by adding a gurney flap. However, the influence of airfoil performance by gurney flap depends on the mounting angle size used. The average percentage increase in the C_l value for the gurney flap with a 45° mounting angle is 23%, with the maximum lift point obtained at AoA 11°, while the flap set at a 60° mounting angle enhances the C_l value by 28% with the maximum lift point at AoA 10°, and for gurney flaps with a 90° mounting angle can increase the C_l value by 45% with maximum lift conditions at AoA 11°. Besides that, the use of a gurney flap has the effect of increasing drag as the mounting angle increases. This increase begins to appear at AoA≥15° with the average percentage increase in C_d based on variations in flap size being 3% for gurney flaps with a 45° mounting angle. Then, when the mounting angle size is 60°, there is an increase in drag of 4%, and it increases again to 5% when the mounting angle becomes 90°.

Based on the C_l/C_d curve plot, using a gurney flap with a 90° mounting angle is more recommended than other mounting angle variations. Meanwhile, based on the C_p curve, the distance between the upper and lower chamber airfoil curves influences the C_l value as the size of the mounting angle variation increases. This makes using gurney flaps with varying mounting angles effective in producing the highest C_l value at a mounting angle of 90°. Furthermore, the analysis of velocity and streamline contours reveals that adding a Gurney flap expands the high-velocity region on the upper airfoil while reducing the velocity on the lower airfoil. However, the streamlined contour does not significantly influence the airfoil as the mounting angle flap increases. Additionally, pressure contour visualization illustrates that the gurney flap causes an addition in lower chamber pressure NACA 0015 and a reduction in the upper chamber NACA 0015, which causes the NACA 0015 to experience an increase in C_l.

REFERENCE

[1] Z. Min, V. K. Kien, and L. J. Y. Richard, "Aircraft morphing wing concepts with radical geometry change," *IES J. Part A Civ. Struct. Eng.*, vol. 3, no. 3, pp. 188–195, 2010.

[2] M. T. I. Gias, M. A. Hossain, M. M. Hasan, and M. Mashud, "Flow separation control on a NACA 0015 airfoil using co-flow jet (CFJ) flow." IEEE, 2014.

[3] M. A. Bin Aziz and M. S. Islam, "Effect of Lower Surface Modification On Aerodynamic Characteristics of an Airfoil," in *International Conference on Mechanical Engineering and Renewable Energy*, 2017.

[4] J. J. Wang, Y. C. Li, and K.-S. Choi, "Gurney flap—Lift enhancement, mechanisms and applications," *Prog. Aerosp. Sci.*, vol. 44, no. 1, pp. 22–47, 2008.

[5] C. P. Van Dam, D. T. Yen, and P. Vijgen, "Gurney flap experiments on airfoil and wings," *J. Aircr.*, vol. 36, no. 2, pp. 484–486, 1999.

[6] U. Fernandez-Gamiz, M. Gomez-Mármol, and T. Chacón-Rebollo, "Computational modeling of gurney flaps and microtabs by POD method," *Energies*, vol. 11, no. 8, p. 2091, 2018.

[7] S. Mubassira, F. I. Muna, and M. I. Inam, "Numerical Investigation of Aerodynamic Characteristics of NACA 4312 Airfoil with Gurney Flap," *J. Eng. Adv.*, vol. 2, no. 02, pp. 63–70, 2021.

[8] M. A. Woodgate, V. A. Pastrikakis, and G. N. Barakos, "Rotor computations with active gurney flaps," in *Advances in Fluid-Structure Interaction: Updated contributions reflecting new findings presented at the ERCOFTAC Symposium on Unsteady Separation in Fluid-Structure Interaction, 17-21 June 2013, St John Resort, Mykonos, Greece*, 2016, pp. 133–166.

[9] R. H. Liebeck, "Design of subsonic airfoils for high lift," *J. Aircr.*, vol. 15, no. 9, pp. 547–561, 1978.

[10] B. L. Storms and C. S. Jang, "Lift enhancement of an airfoil using a Gurney flap and vortex generators," *J. Aircr.*, vol. 31, no. 3, pp. 542–547, 1994.

[11] S. Jain, N. Sitaram, and S. Krishnaswamy, "Computational investigations on the effects of Gurney flap on airfoil aerodynamics," *Int. Sch. Res. Not.*, vol. 2015, 2015.

[12] A. Kumar, P. Chaubdar, G. S. Sinha, and A. B. Harichandan,

"Performance Analysis of NACA4412 Airfoil with Gurney Flap," in *Proceedings of International Conference on Thermofluids: KIIT Thermo 2020*, 2020, pp. 167–176.

[13] P. D. Abd Aziz, A. K. R. Mohamad, F. Z. Hamidon, N. Mohamad, N. Salleh, and N. M. Yunus, "A simulation study on airfoils using VAWT design for low wind speed application," in *2014 4th International Conference on Engineering Technology and Technopreneuship (ICE2T)*, 2014, pp. 105–109.

[14] R. I. Rubel, M. K. Uddin, M. Z. Islam, and M. D. Rokunuzzaman, "Numerical and experimental investigation of aerodynamics characteristics of NACA 0015 aerofoil," *Int. J. Eng. Technol. IJET*, vol. 2, no. 4, pp. 132–141, 2016.

[15] S. M. A. Aftab, A. S. Mohd Rafie, N. A. Razak, and K. A. Ahmad, "Turbulence model selection for low Reynolds number flows," *PLoS One*, vol. 11, no. 4, p. e0153755, 2016, [Online]. Available: https://doi.org/10.1371/journal.pone.0153755

[16] A. J. Lew, G. C. Buscaglia, and P. M. Carrica, "A note on the numerical treatment of the k-epsilon turbulence model," *Int. J. Comut. Fluid Dyn.*, vol. 14, no. 3, pp. 201–209, 2001.

[17] T. Tamura and T. Miyagi, "The effect of turbulence on aerodynamic forces on a square cylinder with various corner shapes," *J. Wind Eng. Ind. Aerodyn.*, vol. 83, no. 1–3, pp. 135–145, 1999, [Online]. Available: https://doi.org/10.1016/S0167-6105(99)00067-7

[18] P. J. Roache, "Perspective: a method for uniform reporting of grid refinement studies," 1994.

[19] J. Julian, R. A. Anggara, and F. Wahyuni, "Influence of Slat Size Variation as Passive Flow Control Instruments on NACA 4415 Airfoil Toward Aerodynamic Performance," *Int. J. Mar. Eng. Innov. Res.*, vol. 8, no. 2, 2023.

[20] J. Julian, W. Iskandar, and F. Wahyuni, "Leading Edge Modification of NACA 0015 and NACA 4415 Inspired by Beluga Whale," *Int. J. Mar. Eng. Innov. Res.*, vol. 8, no. 2, 2023.

[21] P. Kekina and C. Suvanjumrat, "A comparative study on turbulence models for simulation of flow past naca 0015 airfoil using openfoam," in *MATEC web of conferences*, 2017, vol. 95, p. 12005.

[22] C. Çıtak, "Wave drag optimization of high speed aircraft." Middle East Technical University, 2015.